

THz Surface Plasmons in Wide and Freestanding Graphene Nanoribbon Arrays

Talia Tene ¹, Marco Guevara ², Yesenia Cevallos ³, Miguel Ángel Sáez Paguay ⁴, Stefano Bellucci ⁵ and Cristian Vacacela Gomez ^{6,*}

¹ Department of Chemistry, Universidad Técnica Particular de Loja, Loja 110160, Ecuador; tbtene@utpl.edu.ec

² Faculty of Mechanical Engineering, Escuela Superior Politécnica de Chimborazo (ESPOCH), Riobamba 060155, Ecuador

³ College of Engineering, Universidad Nacional de Chimborazo, Riobamba 060108, Ecuador;

⁴ Facultad de Recursos Naturales, Escuela Superior Politécnica de Chimborazo (ESPOCH), Orellana 220201, Ecuador

⁵ INFN-Laboratori Nazionali di Frascati, Via E. Fermi 54, I-00044 Frascati, RM, Italy;

⁶ UNICARIBE Research Center, University of Calabria, I-87036 Rende, CS, Italy

* Correspondence: cristianisaac.vacacelagomez@fis.unical.it

Citation: Tene, T.; Guevara, M.; Cevallos, Y.; Sáez Paguay, M.Á.; Bellucci, S.; Vacacela Gomez, C. THz Surface Plasmons in Wide and Freestanding Graphene Nanoribbon Arrays. *Coatings* **2023**, *13*, 28. <https://doi.org/10.3390/coatings13010028>

Academic Editor: Marcin Pisarek

Received: 18 November 2022

Revised: 8 December 2022

Accepted: 20 December 2022

Published: 23 December 2022



Copyright: © 2022 by the authors. Licensee MDPI, Basel, Switzerland. This article is an open access article distributed under the terms and conditions of the Creative Commons Attribution (CC BY) license (<https://creativecommons.org/licenses/by/4.0/>).

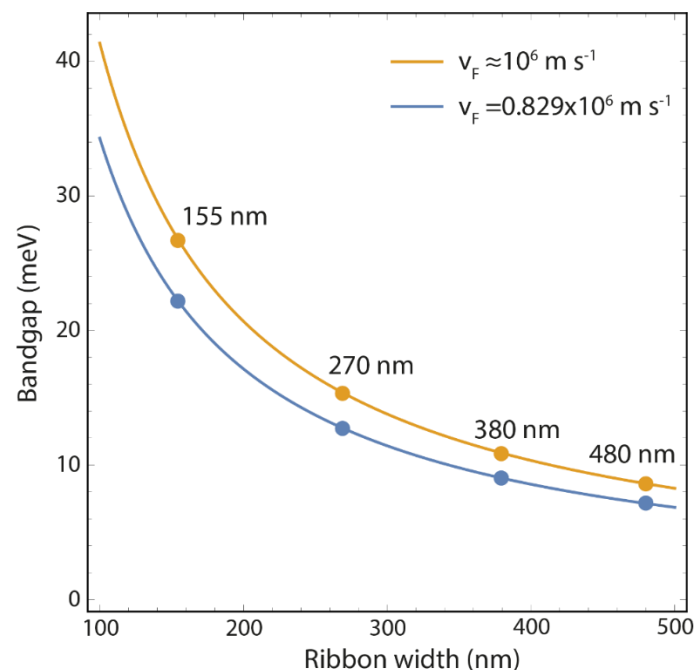


Figure S1. Bandgap (Δ) as a function of the ribbon width (w), considering the charge carrier velocity computed by DFT-LDA ($v_F = 0.829 \times 10^6 \text{ m/s}$) (Ref. [25] in the main text) and the conventional value widely used ($v_F \approx 10^6 \text{ m/s}$) (Ref. [28] in the main text). Markers represent the GNR systems under study and continue lines are the fitting curve using Equation 2 (in the main text).

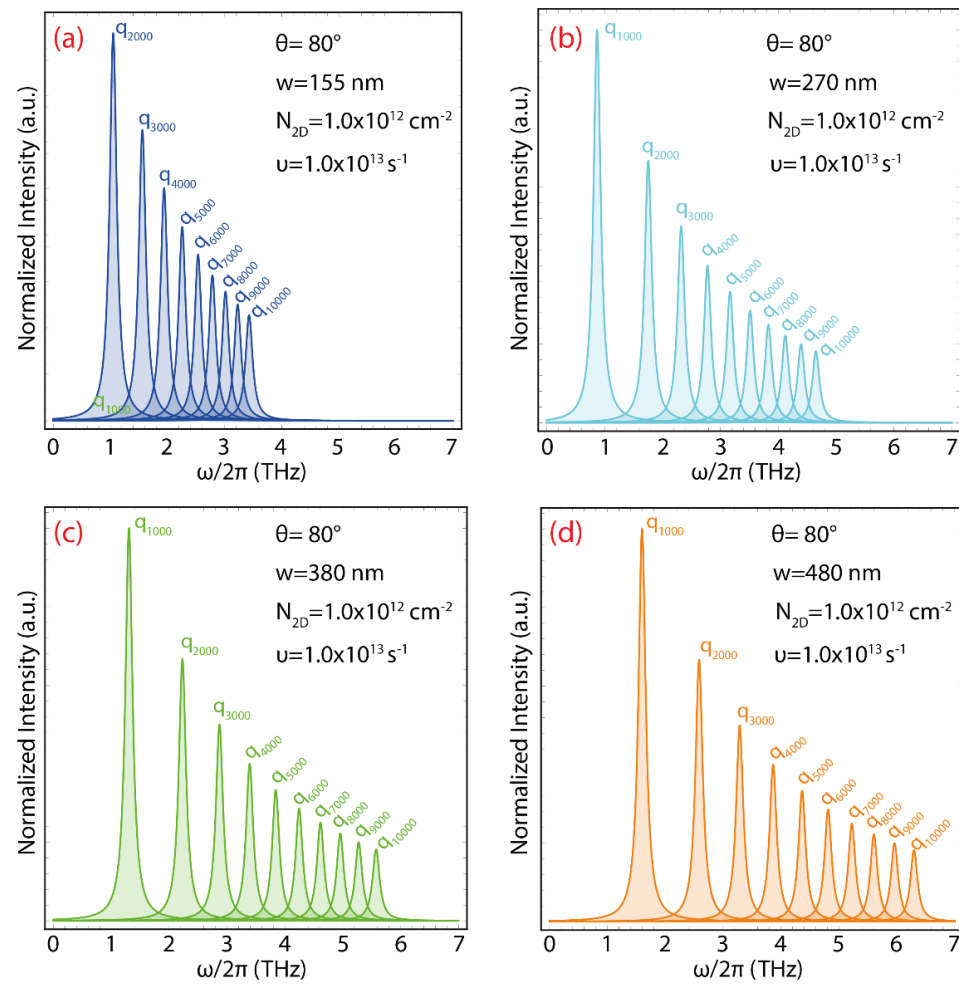


Figure S2. Plasmon frequency ($\omega/2\pi \leq 7 \text{ THz}$) (using $\theta = 80^\circ$, $N_{2D} = 1.0 \times 10^{12} \text{ cm}^{-2}$, $\nu = 1.0 \times 10^{13} \text{ s}^{-1}$, and $v_F = 0.829 \times 10^6 \text{ m/s}$) for selected q values from 1000 to 10,000 cm^{-1} , with different ribbon widths: (a) $w = 155 \text{ nm}$, (b) $w = 270 \text{ nm}$, (c) $w = 380 \text{ nm}$, and (d) $w = 480 \text{ nm}$. Plasmon spectra were constructed using the Lorentz line shape function to a maximum value of 1, setting the full width at half maximum to 0.2, and the corresponding transition frequency was taken from Table 4 (in the main text) for the selected q values. A conventional exponential decay function is adopted for the dispersion of the plasmon spectra.

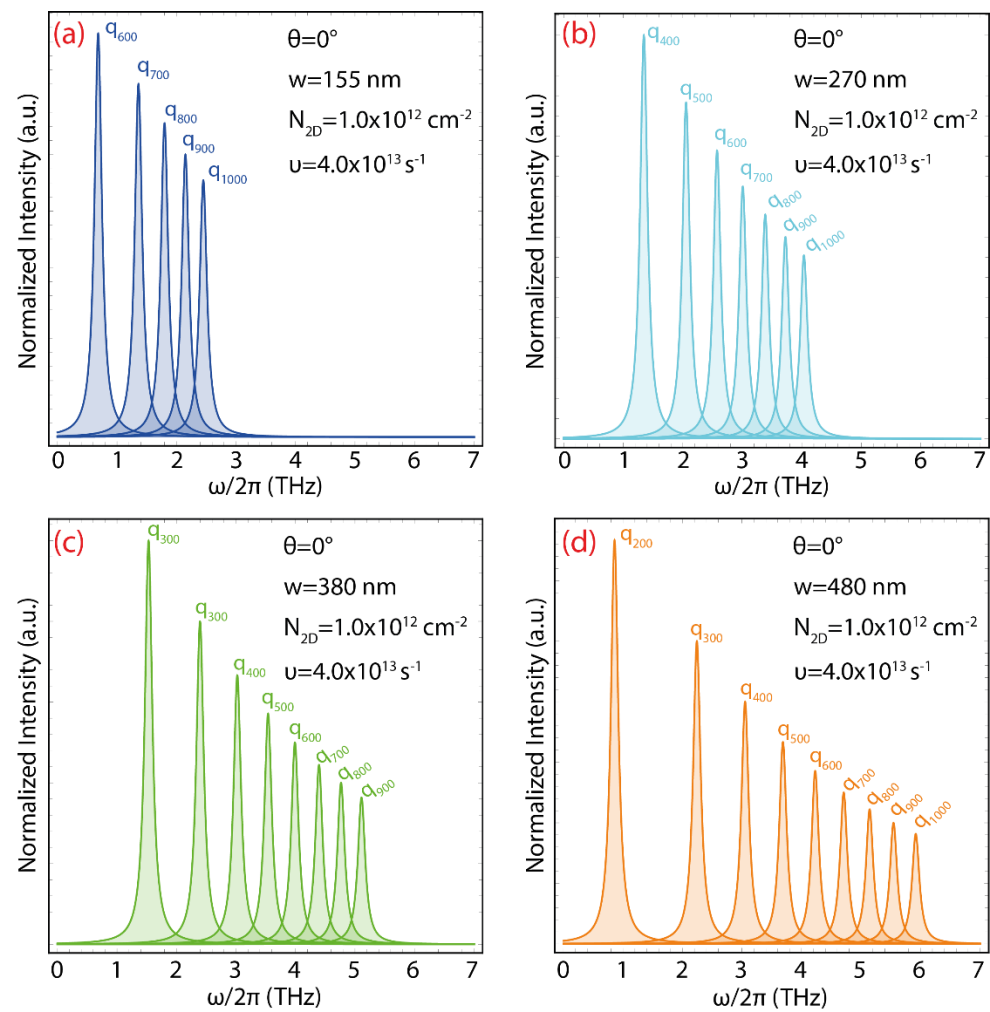


Figure S3. Plasmon frequency ($\omega/2\pi \leq 7 \text{ THz}$) (using $\theta = 0$, $N_{2D} = 1.0 \times 10^{12} \text{ cm}^{-2}$, $\nu = 4.0 \times 10^{13} \text{ s}^{-1}$, and $v_F = 0.829 \times 10^6 \text{ m/s}$) for selected q values from 100 to 1000 cm^{-1} , with different ribbon widths: (a) $w = 155 \text{ nm}$, (b) $w = 270 \text{ nm}$, (c) $w = 380 \text{ nm}$, and (d) $w = 480 \text{ nm}$. Plasmon spectra were constructed using the Lorentz line shape function to a maximum value of 1, setting the full width at half maximum to 0.2, and the corresponding transition frequency was taken from Table 6 (in the main text) for the selected q values. A conventional exponential decay function is adopted for the dispersion of the plasmon spectra.

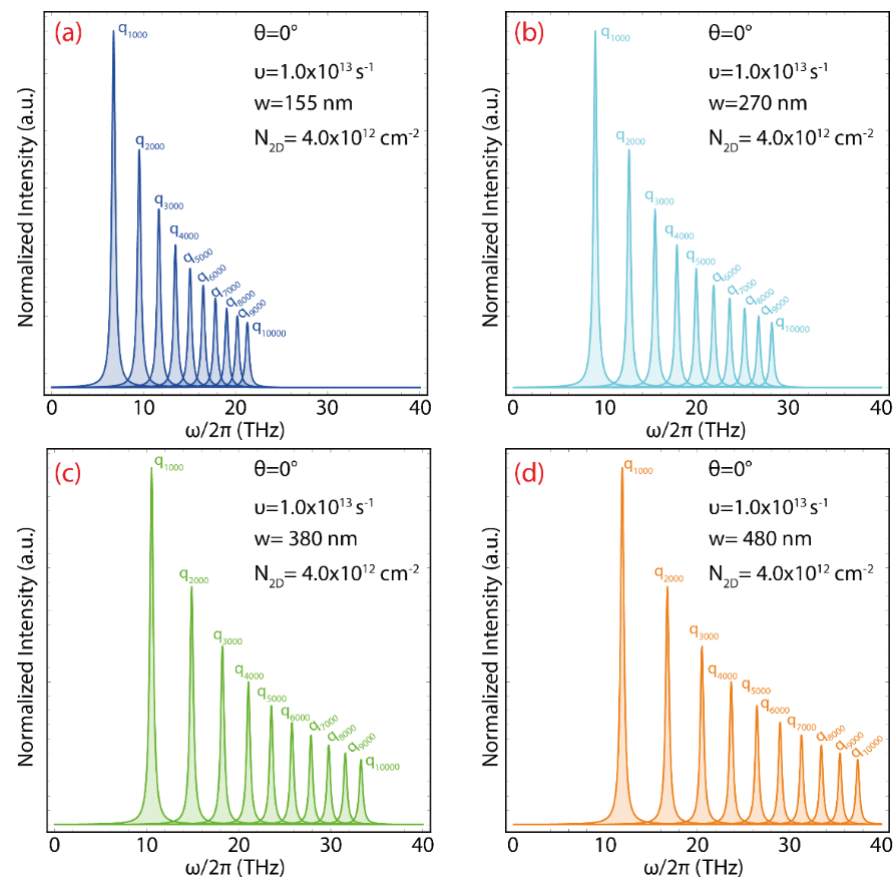


Figure S4. Plasmon frequency ($\omega/2\pi \leq 40$ THz) (using $\theta = 0$, $N_{2D} = 4.0 \times 10^{12} \text{ cm}^{-2}$, $\nu = 1.0 \times 10^{13} \text{ s}^{-1}$, and $v_F = 0.829 \times 10^6 \text{ m/s}$) for selected q values from 1000 to 10,000 cm^{-1} , with different ribbon widths: (a) $w = 155 \text{ nm}$, (b) $w = 270 \text{ nm}$, (c) $w = 380 \text{ nm}$, and (c) $w = 480 \text{ nm}$. Plasmon spectra were constructed using the Lorentz line shape function to a maximum value of 1, setting the full width at half maximum to 0.2, and the corresponding transition frequency was taken from Table 8 (in the main text) for the selected q values. A conventional exponential decay function is adopted for the dispersion of the plasmon spectra.

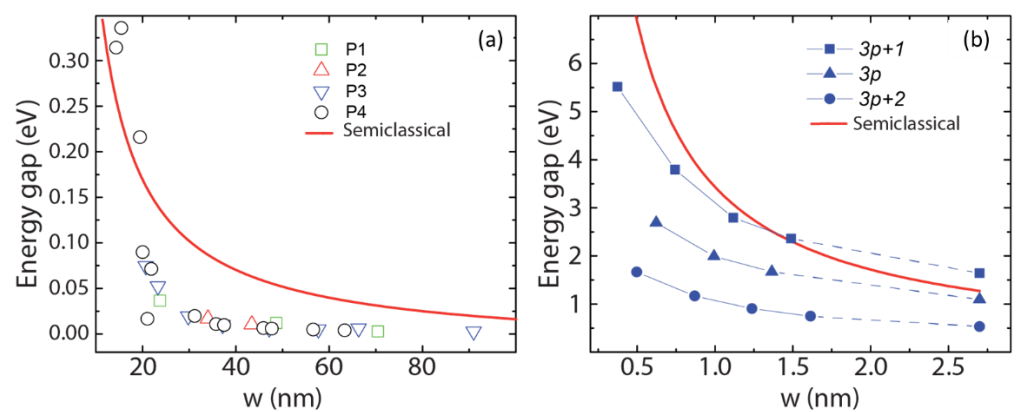


Figure S5. Bandgap as a function of ribbon width. (a) Experimental results for different datasets (P1-P4) and (b) GW approximation for different families of GNRs (Ref. [29] in the main text). The red line is the predicted curve using Equation (2) (in the main text).

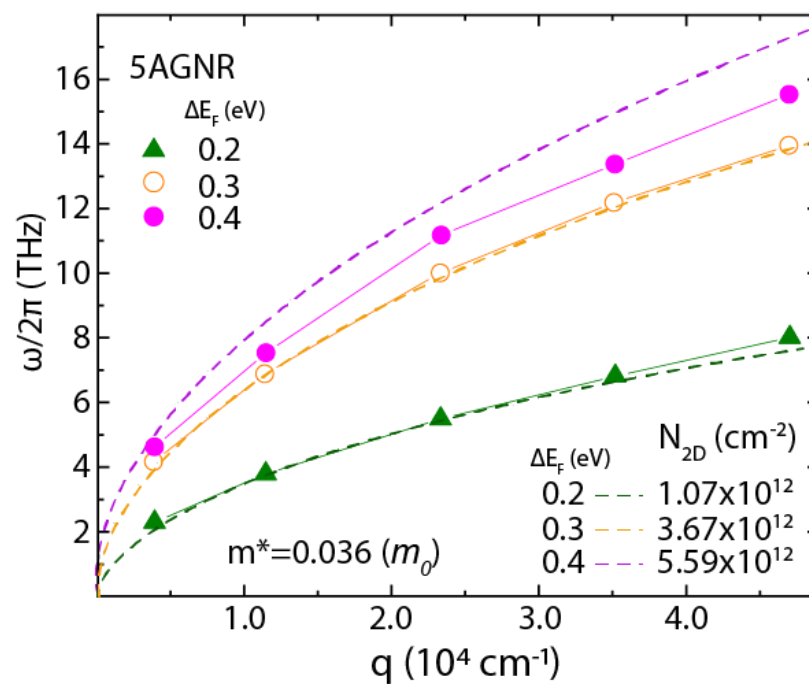


Figure S6. Plasmon frequency dispersion ($\omega/2\pi$) vs. wave vector (q) for five armchair graphene nanoribbon (5AGNR), considering the numerical TDDFT+RPA approach (Ref. [20] in the main text) and the predictions of the semi-analytical model through Equation (4). The input parameters of Equation (4) are given in the figure.